

Supplementary Material

Gelatin Nanoparticle-Coated Silicon Beads for Density-Selective Capture and Release of Heterogeneous Circulating Tumor Cell with High Purity

Qinqin Huang^{1,2,6}, Fu-Bing Wang³, Chun-Hui Yuan³, Zhaobo He², Lang Rao², Bo Cai², Bolei Chen⁵, Susu Jiang^{1,6}, Zhiqiang Li¹, Jincao Chen¹, Wei Liu², Feng Guo⁴, Zheng Ao⁴✉, Shi Chen^{1,6}✉ and Xing-Zhong Zhao²✉

1. Brain Center, Zhongnan Hospital, Wuhan University, Wuhan 430072, China.
2. Key Laboratory of Artificial Micro- and Nano-Structures of Ministry of Education, School of Physics and Technology, Wuhan University, Wuhan 430072, China.
3. Department of Laboratory Medicine, Zhongnan Hospital of Wuhan University, Wuhan 430071, China.
4. Department of Intelligent Systems Engineering, Indiana University, Bloomington, IN 47405, USA.
5. Institute for Interdisciplinary Research, Jiangnan University, Wuhan 430056, China.
6. Key Laboratory of Combinatorial Biosynthesis and Drug Discovery of Ministry of Education, School of Pharmaceutical Sciences, Wuhan University, Wuhan 430072, China.

✉Corresponding authors: Shi Chen (shichen@whu.edu.cn), Zheng Ao (zheng.ao@sri.com), Xing-Zhong Zhao (xzzhao@whu.edu.cn)

This file includes:

Supplementary Figure S1 – 10

Materials

Paraformaldehyde (PFA, 36% in water), Triton X-100, bovine serum albumin (BSA), Propidium iodide (PI), carboxy-fluorescein succinimidyl ester (CFSE), normal goat serum, 4, 6-diamidino-2-phenylindole dihydrochloride (DAPI), 3-Aminopropyltriethoxysilane (APS), Gelatin type A (175 bloom) from pork skin, glutaraldehyde solution (Grade I, 50%), matrix metalloproteinase-9 (MMP-9) and Percoll solution (1.13 g mL^{-1}) were obtained from Sigma-Aldrich. Dulbecco's modified Eagle's medium (DMEM, Hyclone, high glucose) and phosphate buffer solution (PBS, PH=7.4) were obtained from Thermo-Fisher Scientific. Streptavidin (SA), Tween-20, fetal bovine serum (FBS) and 0.25 % Trypsin-EDTA (Gibco, 1X) were obtained from Invitrogen (Carlsbad, CA). Biotinylated monoclonal anti-human EpCAM/TROP1 antibody (Goat IgG) was obtained from R&D systems. Phycoerythrin (PE)-labeled anti-cytokeratin (CAM5.2), fluorescein isothiocyanate (FITC)-labeled anti-human CD45 (Ms IgG1, clone H130) and Phycoerythrin (PE)-labeled anti-human CD146 were purchased from BD Biosciences. Allophycocyanin (APC)-labeled anti-human CD326 (EpCAM) was purchased from Biolegend. Biotinylated monoclonal anti-human CD146 monoclonal antibody was purchased from Miltenyi Biotec. Solid silica microbeads were obtained from Suzhou Knowledge & Benefit Sphere Tech. Co., Ltd.

Preparation and characterization of SiO₂@Gel MBs

Silica microbeads (0.1 g) were dispersed in ethanol (50 mL), which was followed by the addition of 3-aminopropyltriethoxysilane (APTES) (0.2 mL). The mixture was gently stirred for 3 h at 50 °C to obtain amino-modified silica microbeads (SiO₂-NH₂). The

precipitate was centrifuged and washed several times with ethanol and then deionized water. Next, SiO₂-NH₂ MBs were redispersed in deionized water and mixed with 0.2 mL of glutaraldehyde (GA, 50% content in H₂O). The mixture was stirred at room temperature for 10 h to obtain aldehyde-modified silica microbeads (SiO₂-CHO) and then centrifuged to remove excess GA solution. Gelatin solution (1% in water, type A, 175 bloom) was slowly added to cross-link the aldehyde-functionalized microbeads for 4 h via the formation of Schiff-base bonds between residual aldehyde groups on the surface of the microspheres and amine groups of the gelatin. Then, 4 °C deionized water (50 mL) was poured into the mixture rapidly. After removal of excess gelatin by centrifugation, the resulting SiO₂@Gel MBs were re-suspended and stored in 1% BSA for further experiments.

The coating of gelatin nanoparticles on silica microbeads was measured by SEM (6700F, JEOL, Japan), TEM (JEM-2010 ES500W, Japan, operated at 30 kV), and FTIR (5700, Thermo Nicolet, USA) and XRD (X'Pert Pro X-ray diffractometer, PANalytical) spectroscopy. The FTIR and XRD spectra of silica, gelatin nanoparticle-coated silica, and gelatin alone are presented in Figure. S1A,B. The FTIR spectrum of SiO₂@Gel MBs showed an absorption band at approximately 1635 cm⁻¹, which corresponds to N-H stretching vibrations of gelatin; bare MBs had no adsorption at that wavenumber. The XRD patterns showed that all biomaterials were in amorphous states, and the diffraction angle center of SiO₂@Gel (2θ 21.7°) was slightly sharpened and shifted from the diffraction angle of silica (2θ 22.8°). The diameter of MBs was analyzed using Image-Pro Plus 6.0 software.

Surface modification of SiO₂@Gel MBs

A 100 μL SiO₂@Gel MBs aqueous solution (suspended in 0.1 M MES) was mixed with 200 μL of EDC (4 mg mL⁻¹ in 0.1 M MES buffer)/NHS (6 mg mL⁻¹ in 0.1 M MES buffer) at room temperature for 30 min to activate the carboxyl groups on the surfaces of the gelatin coating. After the mixed solution was washed with PBS three times, streptavidin (SA, 50 $\mu\text{g mL}^{-1}$ in PBS) was added to the microbeads for 10 h at 4 $^{\circ}\text{C}$. Subsequently, protein G in PBS was added to improve the orientation of anti-EpCAM, and the tube was shaken for 2 h. After being washed with PBS, the microbeads were treated with biotinylated anti-EpCAM (10 $\mu\text{g mL}^{-1}$ in PBS) and/or anti-CD146 (10 $\mu\text{g mL}^{-1}$ in BSA) for another 2 h at room temperature to direct these antibodies onto microbead surfaces.

Supplementary Figures

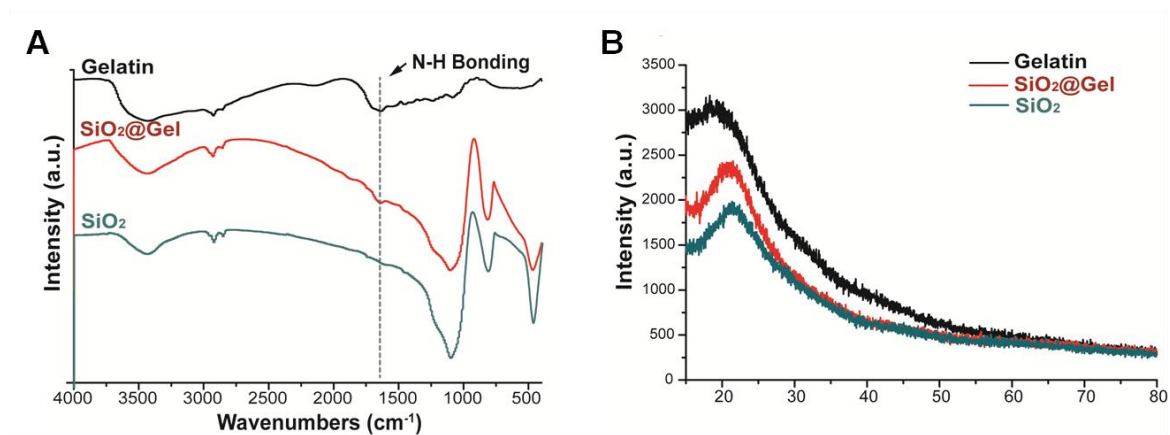


Figure S1. Characterization of gelatin nanoparticle-coated silica microbeads. **(A)** Fourier transform infrared (FTIR) spectra, and **(B)** X-ray diffraction (XRD) spectra of gelatin, SiO_2 MBs and SiO_2 @Gel MBs.

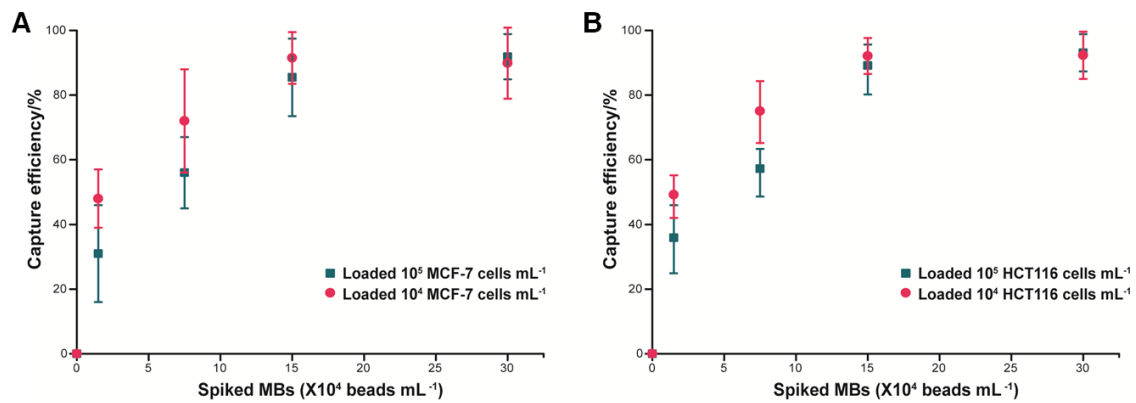


Figure S2. Evaluation of cell-capture efficiency for (A) MCF-7 ($10^4/10^5$ cells mL⁻¹ in DMEM) and (B) HCT116 ($10^4/10^5$ cells mL⁻¹ in DMEM) with different bead concentrations. Error bars represent the standard deviations ($n \geq 3$).

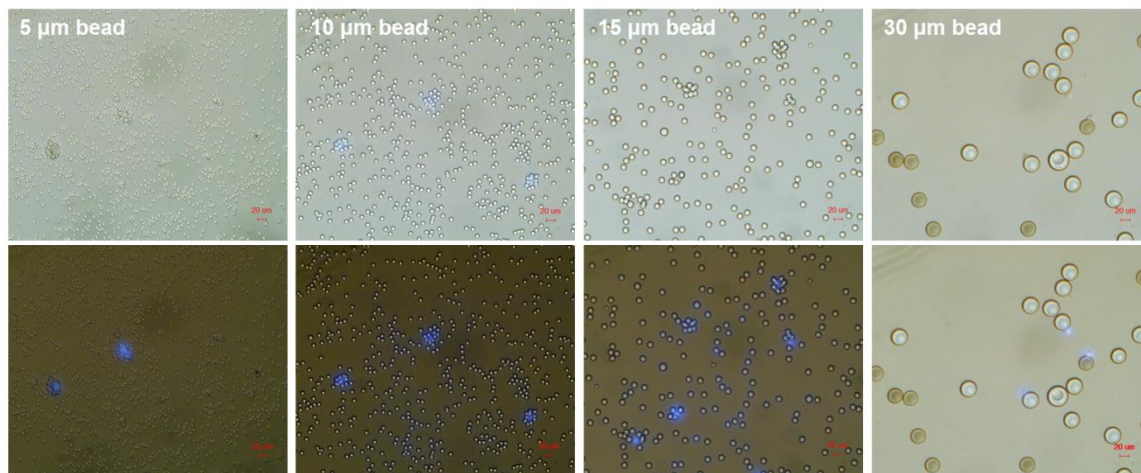


Figure S3. The bright-field (top) and corresponding fluorescence images (bottom) of MCF-7 cells covered with 5, 10, 15, or 30 μm SiO_2 @Gel MBs. Captured cells were identified by DAPI staining (blue). The scale bars are 20 μm .

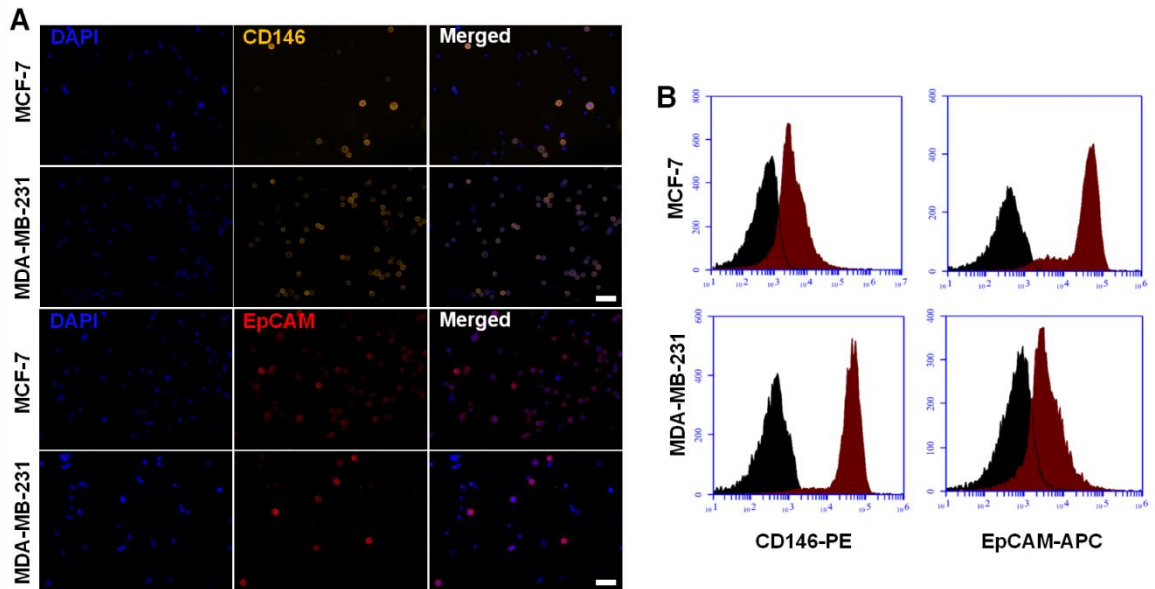


Figure S4. (A) Immunofluorescence images of MCF-7 and MDA-MB-231 cells labeled with DAPI (blue), anti-CD146-PE (yellow) alone, or anti-EpCAM-APC (red) alone, respectively. Scale bar is 50 μm . (B) Quantitation of CD146 and EpCAM expression in two cell lines using flow cytometry, followed by stained with PE-labeled anti-CD146 and APC-labeled anti-EpCAM for 10 min. Black histograms show unstained cells, red histograms show expression on CD146-stained cells (left panel) and EpCAM-stained cells (right panel). A minimum of 10^5 cells were analyzed for each sample.

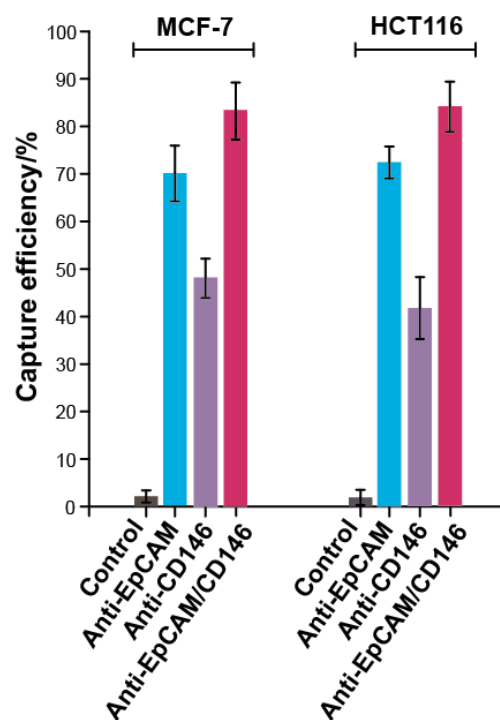


Figure S5. Comparison of the capture efficiency of cancer cells (MCF-7 and HCT116) using SiO₂@Gel MBs without antibody coating, only the anti-EpCAM coating, only the anti-CD146 coating, and both the anti-EpCAM and anti-CD146 coatings. Cell suspensions (1 mL in DMEM) containing MCF-7 (10⁵ cells) or HCT116 (10⁵ cells) were employed as model systems. Error bars represent the standard deviations (n≥3).

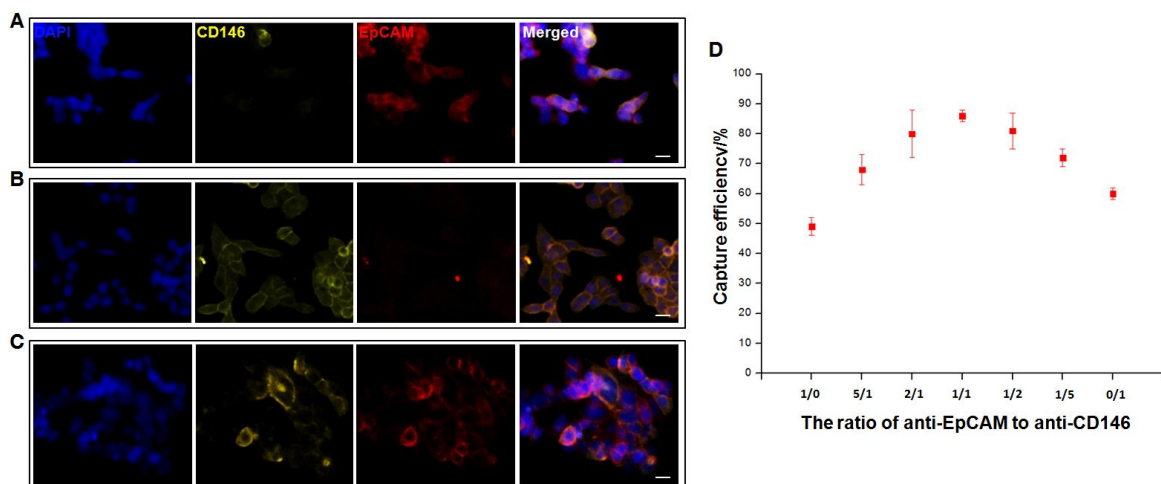


Figure S6. (A-C) Confocal microscope images of cancer cells (i.e., MCF-7 and MDA-MB-231 cell lines) isolated using SiO₂@Gel MBs coated with different ratios of anti-EpCAM and anti-CD146 (a, 5/1; b, 1/5; and c, 1/1). Cells were released and treated with DAPI, PE-anti-CD146, and APC-anti-EpCAM, followed by 2 h of incubation at 37 °C. Cell suspensions (1 mL in DMEM) containing MCF-7 (10⁴ cells) and MDA-MB-231 (10⁴ cells) were employed as model systems. The scale bars are 20 μm. (D) Comparison of the capture efficiency of cancer cells using SiO₂@Gel MBs coated with different ratios of anti-EpCAM and anti-CD146 (i.e., 1/0, 5/1, 2/1, 1/1, 1/2, 1/5 and 0/1). Error bars represent the standard deviations (n ≥ 3).

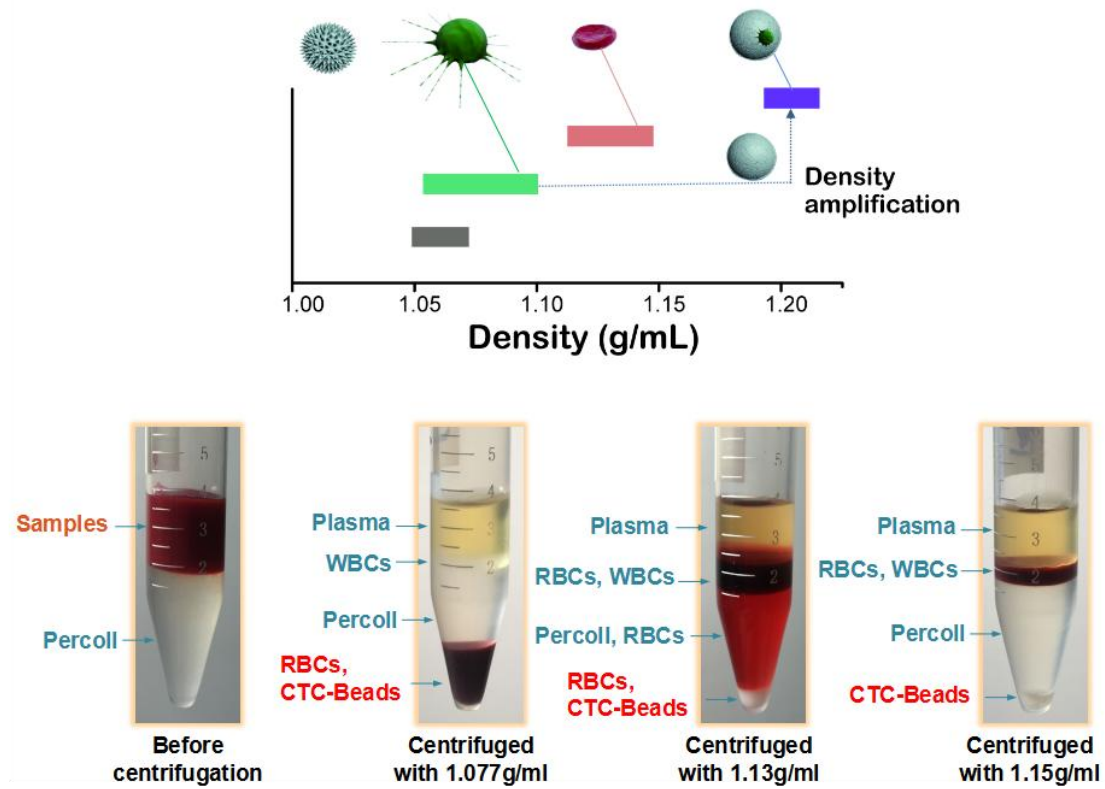


Figure S7. Photographs of centrifuge tubes before and after centrifugation using different densities of Percoll medium (1.077, 1.13 and 1.15 g mL⁻¹) at 400×g for 10 min.

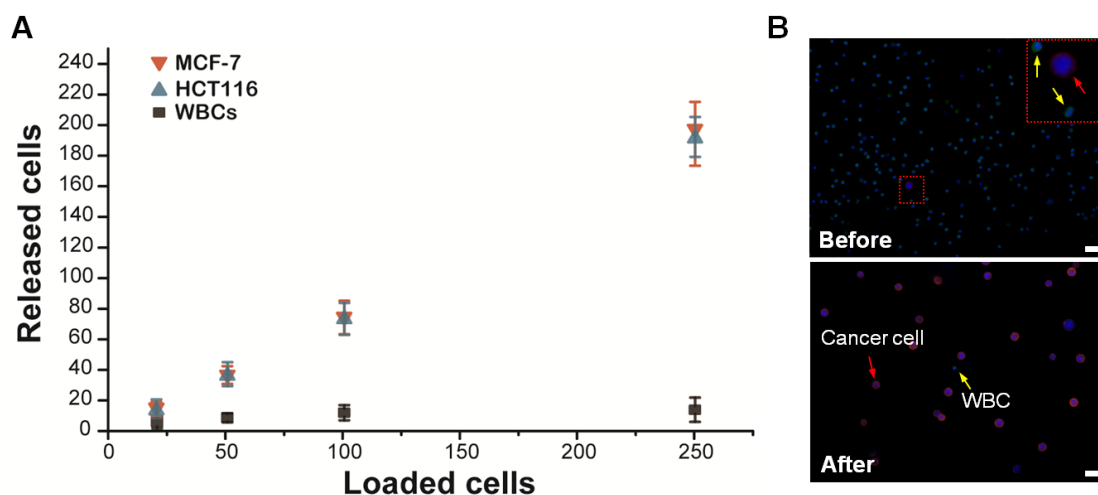


Figure S8. Purification of cancer cells (MCF-7 and HCT116) at different cell numbers from whole blood. **(A)** Release performance of specifically captured cancer cells (MCF-7 and HCT116) and non-specifically bonded WBCs on the surface of SiO₂@Gel MBs via the MMP-9 induced gelatin degradation. Error bars represent the standard deviations ($n \geq 3$). **(B)** Fluorescence images of cells before (left) and after (right) purification. Red dots (positive for EpCAM) are considered HCT116, whereas green dots (positive for CD45) are considered WBCs. The scale bars are 100 μm (top) and 30 μm (bottom).

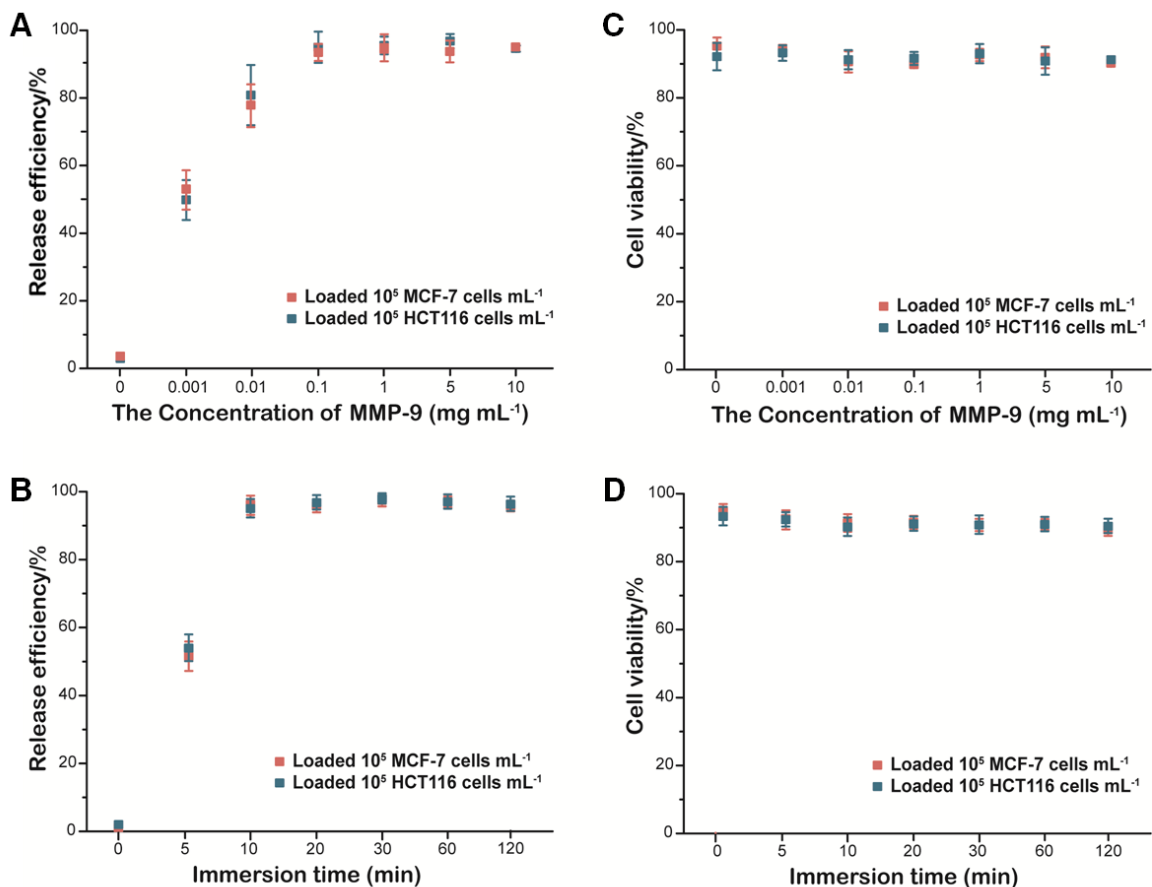


Figure S9. Release efficiency of cancer cells (MCF-7 and HCT116) with (A) different concentrations of MMP-9 solution and at (B) different incubation times. Viability of cancer cells (MCF-7 and HCT116) with (C) different concentrations of MMP-9 solution and at (D) different incubation times. Suspensions (1 mL) of 10⁵ mL⁻¹ MCF-7 cells or HCT116 cells in DMEM were employed as model systems. Error bars represent the standard deviations ($n \geq 3$).

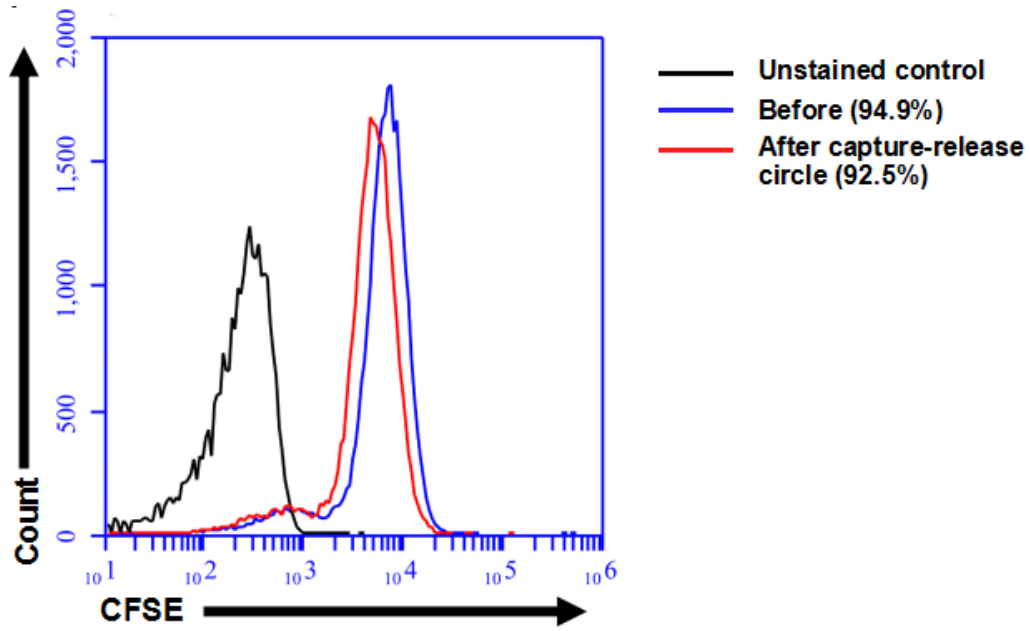


Figure S10. Evaluation of cell viability. Flow cytometric analysis of the cell viability. MCF-7 cells (10^6 cells in PBS) were stained with CFSE/PI. The red line shows the captured and released cells, the blue line shows the control cells, and the black line shows the unstained cells.